Supplemental Document

Optics Letters

Large near-infrared lateral photovoltaic effect in an organic egg albumin/Si structure: supplement

XINHUI ZHAO,[1,2] RENZHI WANG,[1,2] PENG BAO,[1,2] YIRU NIU,[1,2] DIYUAN ZHENG,[1,2] ZHUYIKANG ZHAO,[1,2] NAN SU,[1,2] CHENHUA HU,[1,2] SU HU,[1,2] YING WANG,[3] AND HUI WANG[1,2,*]

[1]*State Key Laboratory of Advanced Optical Communication Systems and Networks, School of Physics and Astronomy, Shanghai Jiao Tong University, 800 Dongchuan Road, Shanghai 200240, China*
[2]*Key Laboratory for Thin Film and Microfabrication Technology of the Ministry of Education, Research Institute of Micro/Nano Science and Technology, Shanghai Jiao Tong University, 800 Dongchuan Road, Shanghai 200240, China*
[3]*Center for Advanced Electronic Materials and Devices, School of Electronic Information and Electrical Engineering, Shanghai Jiao Tong University, 800 Dongchuan Road, Shanghai 200240, China*
[*]*Corresponding author:* huiwang@sjtu.edu.cn

Supplement DOI: https://doi.org/10.6084/m9.figshare.20358990

Parent Article DOI: https://doi.org/10.1364/OL.465495

Large near-infrared lateral photovoltaic effect in organic egg albumin/Si structure: supplemental document

1. The fabrication and measurement details of the LPE device.

All the chemicals used in this experiment except chicken eggs were without further purification and deionized water was applied to all the experiments. EA was obtained from fresh chicken eggs randomly selected from the supermarket. A precleaned chicken egg was broken and was put in the culture dish. Then the EA was separated with egg yolk by a stainless-steel mesh spoon. 1 mL EA was diluted with 5 mL deionized water and then sonicated for 2 min to make the EA thoroughly dispersed. The suspended solids of the mixture were removed with a dust-free cloth.

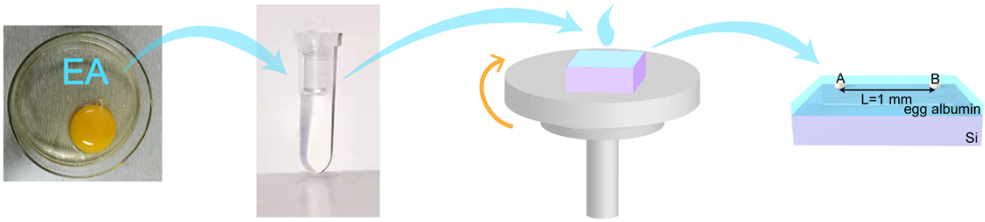

Fig. S1. The fabrication process of the EA/Si device.

The substrates used in this experiment are p-type Si (1 1 1) wafers (thickness ~ 0.35 mm and resistivity ~ 3-6 Ω). It was cleaned in acetone, ethyl alcohol, and deionized water successively using the ultrasonic bath. The prepared EA solution was spin-coated onto Si substrate at different rotate speeds to obtain different thicknesses. And then the device was baked at 65 ^{o}C for 10 min.

The morphology of the EA film was characterized by field emission scanning electron microscopy (FE-SEM, Carl Zeiss Ultra 55, Germany) operating at 5 kV. An energy dispersive spectrometer (EDS) was used to measure the elements composition of the EA film. The LPE performance was measured using a digital multimeter (34410A 6 1/2 Digit Multimeter, Agilent) in ambient condition at room temperature (~ 25±1 ^{o}C) and the position of the laser spot was controlled by a precise translation system. The distance of the two electrodes formed by alloying indium was 1 mm. The surface of the devices was scanned spatially with a semiconductor laser of 10 mW (ranging from visible to near-infrared) focused on a 50 μm diameter spot without any spurious illumination reaching the samples.

2. The characterization of the LPE device.

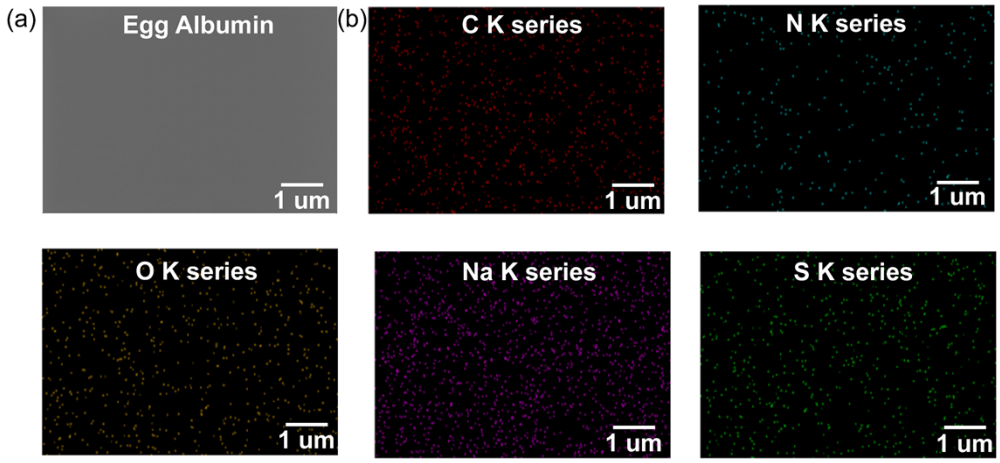

Fig. S2. (a) SEM plane view micrograph of the EA film. (b) EDS maps for the surface of EA film.

In the Fig. S2(a), it can be observed that the surface morphology of EA film is smooth and uniform by spin coating on the Si substrate. The element mapping of energy dispersive spectrometer (EDS) in Fig. S2(b) reveals the presence of elements in EA film. The C, N, O, Na and S peaks appear and the atomic percentage is C of ~ 50.49%, N of ~ 39.01%, O of ~ 9.56% Na of ~ 0.51%. and S of ~ 0.10%.

3.

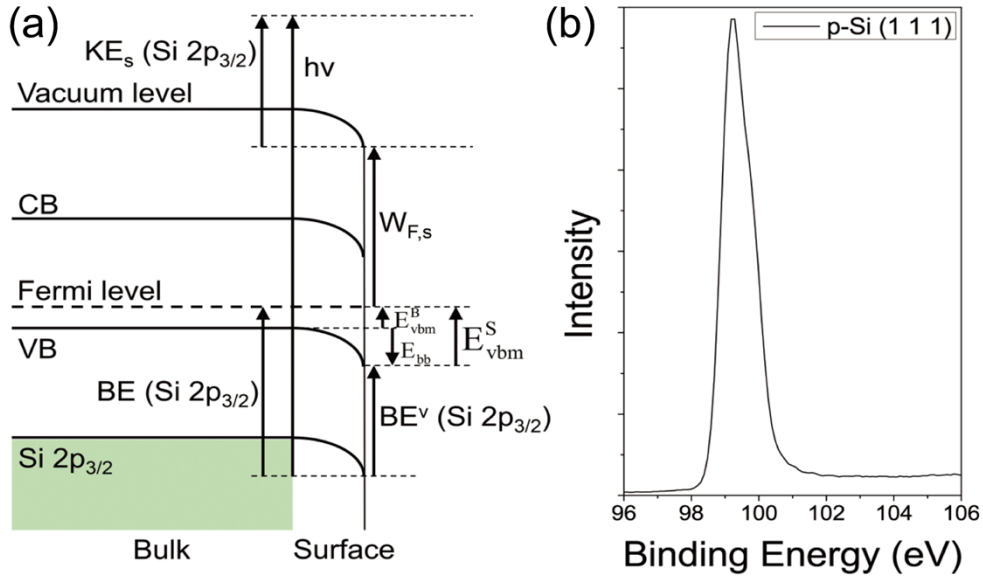

Fig. S3. (a) Schematic energy-level diagram of p-type Si (1 1 1) showing band bending at the surface (Ref. [1], Fig. 2(a)). (b) Si 2p$_{3/2}$ core-level spectra of p-Si (1 1 1). (Ref. [1], Fig. 2(b)).

The surface states could create a space charge region and strong surface band downward bending because of Fermi energy level pinning as shown in Fig.S3(a). Furthermore, the measured binding energy is 99.18 eV, larger than the difference between the calculated bulk Fermi level and the Si $2p_{3/2}$ core level under the flat-band condition. Therefore, the electric field is generated on the surface of p-Si to separate the light-induced carriers as shown in Fig. S3(b).

4.

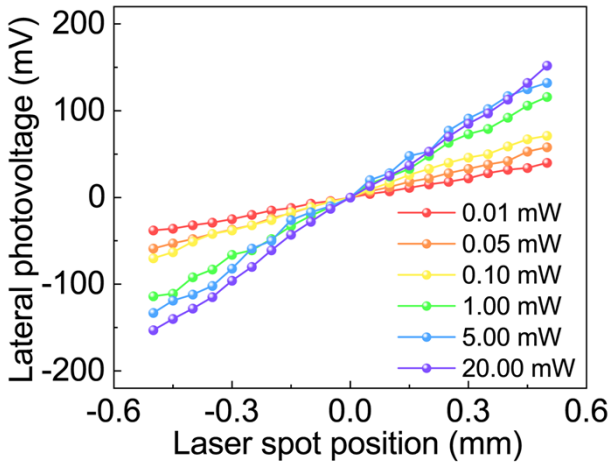

Fig. S4. LPV curve in different laser power under the illumination of 532 nm laser in EA (50 nm)/Si device.

5.

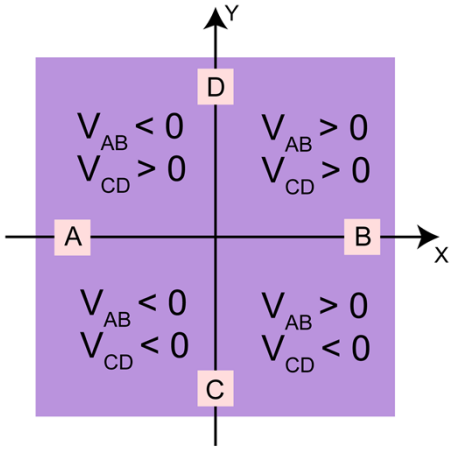

Fig. S5. Full mapping of the LPV on a plane.

6.

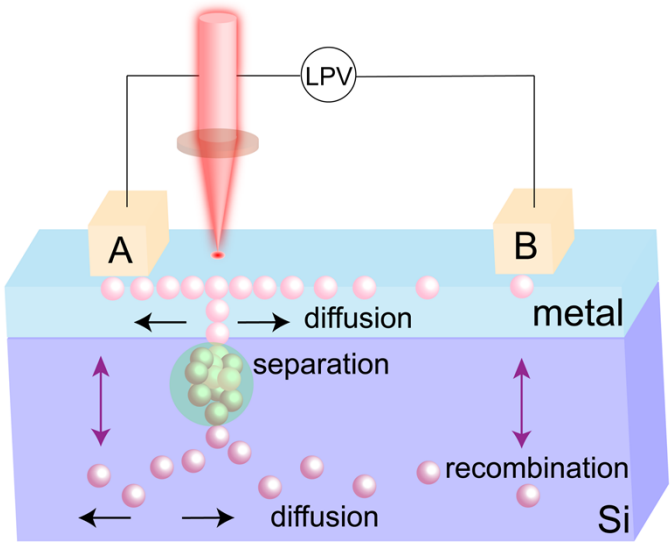

Fig. S6. Schematic of the mechanism of LPE in inorganic structure.

7.

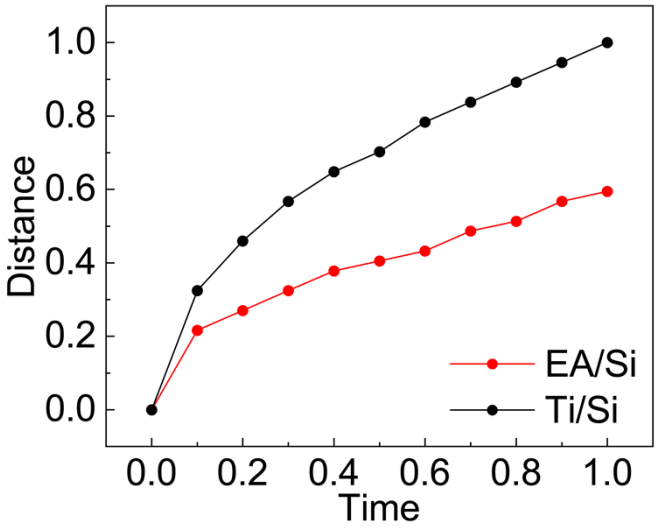

Fig. S7. The comparison of the electron transfer process in EA/Si structure and Ti/Si structure.

7.

Table S1. Performance comparison of the proposed EA/Si device with the reported classic photodetector.

Device	Wavelength (nm)	Laser power (mW)	Sensitivity (mV/mm)	Reference
Fe_3O_4/Si	800	2	32.5	[2]
WS_2/Si	405	10	232	[3]
ZnO/Si	980	5	104.93	[4]
$Bi_2Te_{2.7}Se_{0.3}$/Si	532	30	283.71	[5]
TiO_2/MoS_2/RGO/Si	810	5	15.32	[6]
MoS_2/Si	532	10	329.5	[7]
$MAPbI_3$/Si	532	0.68	50	[8]
EA/Si	980	10	357	This work

8.

Table S2. Performance comparison of the proposed EA/Si device with the reported organic photodetector.

Device	Wavelength range (nm)	Laser power (mW)	Response time (ms)	Recovery time (ms)	Reference
optogenetically engineered living cells	473	230	14.7	5.5	[9]
PSeTPTI/PC 61 BM	UV	/	3.2	0.4	[10]
Carbon Nitride Nanotube Membrane	405-590	50	50	850	[11]
XPL6:PC10BM	320-670	1	3.5	3.1	[12]
Graphene/PTBT/ ODTS/p^+Si	450-750	7.7	7.8	15	[13]

EA/Si	445-980	10	0.30	0.16	This work

References

1. X. Huang, C. Mei, Z. Gan, P. Zhou, and H. Wang, Appl. Phys. Lett. **110**, 1 (2017).

2. X. Wang, B. Song, M. Huo, Y. Song, Z. Lv, Y. Zhang, Y. Wang, Y. Song, J. Wen, Y. Sui, and J. Tang, RSC Adv. **5**, 65048 (2015).

3. D. Zheng, X. Dong, J. Lu, Y. Niu, and H. Wang, Appl. Surf. Sci. **574**, 151662 (2022).

4. X. Dong, D. Zheng, J. Lu, Y. Niu, and H. Wang, Appl. Surf. Sci. **566**, 150687 (2021).

5. S. Qiao, M. Chen, Y. Wang, J. Liu, J. Lu, F. Li, G. Fu, S. Wang, K. Ren, and C. Pan, Adv. Electron. Mater. **5**, 1 (2019).

6. M. Javadi, M. Gholami, and Y. Abdi, J. Mater. Chem. C **6**, 8444 (2018).

7. S. Qiao, J. Liu, G. Fu, S. Wang, K. Ren, and C. Pan, J. Mater. Chem. C **7**, 10642 (2019).

8. A. Z. Ashar, N. Ganesh, and K. S. Narayan, Adv. Electron. Mater. **4**, 2 (2018).

9. J. Yang, G. Li, W. Wang, J. Shi, M. Li, N. Xi, M. Zhang, and L. Liu, Biosens. Bioelectron. **178**, 113050 (2021).

10. Z. Qi, J. Cao, H. Li, L. Ding, and J. Wang, Adv. Funct. Mater. **25**, 3138 (2015).

11. K. Xiao, B. Tu, L. Chen, T. Heil, L. Wen, L. Jiang, and M. Antonietti, Angew. Chemie - Int. Ed. **58**, 12574 (2019).

12. S. Rezaei-Mazinani, A. I. Ivanov, M. Biele, A. L. Rutz, V. G. Gregoriou, A. Avgeropoulos, S. F. Tedde, C. L. Chochos, C. Bernard, R. P. O'Connor, G. G. Malliaras, and E. Ismailova, J. Mater. Chem. C **7**, 9049 (2019).

13. P. H. Chang, Y. C. Tsai, S. W. Shen, S. Y. Liu, K. Y. Huang, C. S. Li, H. P. Chang, and C. I. Wu, ACS Photonics **4**, 2335 (2017).